JOURNAL OF AGRICULTURAL AND FOOD CHEMISTRY

*J. Agric. Food Chem.* **2008,** *56,* 2429–2435 **2429**

# Kinetics of Acid Hydrolysis of Water-Soluble Spruce O-Acetyl Galactoglucomannans

CHUNLIN XU,*,† ANDREY PRANOVICH,† LARI VÄHÄSALO,† JARL HEMMING,† BJARNE HOLMBOM,† HENK A. SCHOLS,‡ AND STEFAN WILLFÖR†

Process Chemistry Centre, Laboratory of Wood and Paper Chemistry, Åbo Akademi University, Porthansgatan 3, FI-20500, Åbo/Turku, Finland, and Agrotechnology and Food Sciences Group, Laboratory of Food Chemistry, University of Wageningen, Bomenweg 2, 6703 HD Wageningen, The Netherlands

Water-soluble *O*-acetyl galactoglucomannan (GGM) is a softwood-derived polysaccharide, which can be extracted on an industrial scale from wood or mechanical pulping waters and now is available in kilogram scale for research and development of value-added products. To develop applications of GGM, information is needed on its stability in acidic conditions. The kinetics of acid hydrolysis of GGM was studied at temperatures up to 90 °C in the pH range of 1–3. Molar mass and molar mass distribution were determined using size exclusion chromatography with multiangle laser light scattering and refractive index detection. The molar mass of GGM decreased considerably with treatment time at temperatures above 70 °C and pH below 2. The molar mass distribution broadened with hydrolysis time. A first-order kinetic model was found to match the acid hydrolysis. The reaction rate constants at various pH values and temperatures were calculated on the basis of the first-order kinetic model. Furthermore, the activation energy, *E*, was obtained from the Arrhenius plot. The activation energy *E* was 150 kJ $mol^{-1}$ for acid hydrolysis of spruce GGM. The apparent rate constant during acid hydrolysis increased by a factor of 10 with a decrease in pH by 1 unit, regardless of temperature. In addition, gas chromatography and matrix-assisted laser desorption/ionization time-of-flight mass spectrometry were applied to study the released GGM monomers and oligomers.

**KEYWORDS: Kinetics; acid hydrolysis; galactoglucomannans; oligosaccharides; stability**

## INTRODUCTION

Mannans currently used in industry are mainly guar gum, konjac glucomannan, locust bean gum, and tara gums. These gums have been applied in the food industry as emulsifiers, thickeners, stabilizers, and gelling agents, as well as in the pharmaceutical, textile, papermaking, and cosmetic industries. Spruce galactoglucomannan (GGM), a potential raw material for hydrocolloids and novel advanced natural materials, is the main hemicellulose type in most softwood species (*1–4*). GGM accounts for 10–20% of the softwood material. Spruce GGM consists of a linear backbone of randomly distributed (1→4)-linked β-D-mannopyranosyl and (1→4)-linked β-D-glucopyranosyl units, with α-D-galactopyranosyl units as single side units to mannosyl units (**Figure 1**) (*2, 5, 6*). The hydroxyl groups at C-2 and C-3 in the mannose units are partially substituted by *O*-acetyl groups (*2, 5, 7*). Spruce GGM can be recovered from process waters in mechanical pulp mills using spruce as raw material and utilized at a competitive cost compared to materials from petrochemicals, for example, ethylene vinyl alcohol, which is currently used as an oxygen barrier in fiber-based packaging materials (*8, 9*). GGM improves the paper properties by sorbing to the fiber surfaces in papermaking (*10*). GGM-based hydrogels and films have also been investigated (*11–13*). Spruce GGM exhibits immunological activity, which makes GGM and its derivatives potentially interesting as biological response modifiers and therapeutic agents (*14*). Recently, we (*15*) have studied the physicochemical properties of spruce GGM solutions. Furthermore, water-soluble Norway spruce GGM has shown promising biological activity and physicochemical properties

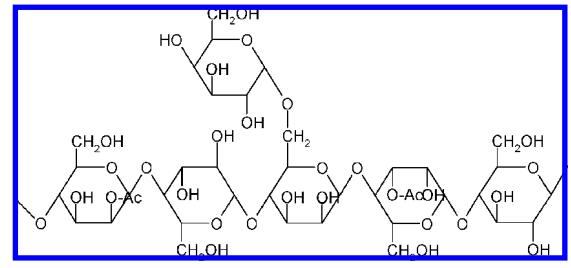


**Figure 1.** Structural features of Norway spruce water-soluble *O*-acetylgalactoglucomannans. Specific features: Gal:Glc:Man ratio ≈ 0.5:1:4; acetyl groups at O-2 and O-3, exclusively in mannosyl units; average molar mass = 21.5 kDa.

* Corresponding author (telephone +358-2-2154888; fax +358-2-2154868; e-mail Chunlin.Xu@abo.fi).
† Åbo Akademi University.
‡ University of Wageningen.

10.1021/jf703702y CCC: $40.75 
Published on Web 03/12/2008

suitable for various applications in, for example, the food, health, papermaking, textile, and cosmetic industries (*4, 14*).

Depolymerization is of great interest in studies of stability and application of natural polymers in the food, paper, pharmaceutical, cosmetic, textile, and oil industries (*16*). In many cases, the application of polymers is dependent not only on their chemical structure but also on a specific molecular size (*17*). Through control of the molecular size, it is possible to control the properties such as viscosity, solubility, and biological activity. Nowadays, there is also a growing interest in developing new routes to manufacturing fuels and chemicals from biomass (*18*). In this process, hydrolysis of polysaccharides is one of the essential steps (*19, 20*). Depolymerization of polysaccharides can be accomplished through chemical, enzymatic, thermal, and ultrasonic processes, which are dependent on the structures and conformation of the polymers, and the reaction medium (*21–25*). In chemical and thermal degradation processes, cleavage of glycosidic bonds in the polysaccharide molecule is the main mechanism for chain scission (*21*). Enzymatic degradation does not obey typical modes of chain scission, because enzymes are considered to be very specific and able to split only specific linkages (*26*). Thermal and ultrasound degradations occur by random scission of glycosidic linkages (*27*). In addition, resulting oligomers from degradation are also possible materials for prebiotic oligosaccharides.

To broaden the application of GGM into food areas, the stability of GGM during recovery, storage, and treatment is of importance. In the present study, we aimed to understand the kinetics of acid hydrolysis of spruce GGM. Hydrolysis of GGM using hydrochloric acid (HCl) was investigated at pH 1, 2, and 3, because the healthy stomach has a pH level of 1−2 by secreting HCl, which rises to 3 or 4 upon digestion of food. Furthermore, this pH range corresponds to the conditions usual for food preparation and storage, where hydrolysis is expected to be a significant reaction (*28*). High-pressure size exclusion chromatography equipped with multiangle laser light scattering and refractive index detectors was applied to measure molar masses and molar mass distributions. The effects of process variables, such as pH value and temperature, were investigated as well.

## MATERIALS AND EXPERIMENTAL PROCEDURES

**Materials.** *O*-Acetyl galactoglucomannan (GGM) was isolated from thermomechanical pulp (TMP) of Norway spruce (*Picea abies*) on large laboratory scale according to the method of Willför et al. (*8*). The GGM water extract was purified and concentrated using different filtration and ultrafiltration techniques. Ethanol with a ratio of 4:1 was added to the concentrated GGM water to precipitate GGM, followed by drying. GGM was further purified by redissolving it in water and performing dialysis. The characteristics of GGM are shown in **Table 1**.

**Hydrolysis.** The GGM solutions were prepared by dissolving the required amount of GGM powder in distilled water at room temperature to make a 0.4 wt % solution. The temperature was then raised to 80 °C and kept constant for 2 h, under continuous stirring with a magnetic stirrer. Finally, the solution was stirred at room temperature overnight. For acid hydrolysis, a certain amount of 1 M HCl was added into 30 mL glass tubes filled with 15 mL of GGM solution to adjust the pH to 1, 2, or 3, respectively, as required. The tubes were sealed with PTFE caps. Hydrolysis was performed in a water bath at temperatures of 90, 70, 50, 37, and 25 °C. After 10 min, 30 min, 1 h, 4 h, 1 day, and 2 days, samples were taken from the water bathes and immediately put into another water bath with a mixture of ice and water. One molar NaOH solution was then added to adjust the pH to 6–7.

**Determination of Molar Mass and Molar Mass Distribution.** Weight-average and number-average molar mass ($M_w$ and $M_n$) and molar mass distribution (MWD) were determined by high-pressure size exclusion chromatography (HPSEC) in online combination with a multiangle laser light scattering (MALLS) instrument (miniDAWN, Wyatt Technology, Santa Barbara, CA) and a refractive index (RI) detector (Shimadzu Corp., Tokyo, Japan). A two-column system, 2× UltrahydrogelTM linear 7.8 × 300 mm column (Waters, Milford, MA), in series was used; 0.1 M $NaNO_3$ was used as the elution solvent. The flow rate was 0.5 mL $min^{-1}$. The samples were filtered through a 0.22 $\mu$m nylon syringe filter before injection. The injection volume was 100 $\mu$L. A d*n*/d*c* value of 0.148 mL $g^{-1}$ was used. Astra software (Wyatt Technology) was used to analyze data.

**Table 1.** Characteristics of GGM

| | GGM |
|---|---|
| sugar composition, mol % | |
| mannose | 66 |
| glucose | 17 |
| galactose | 11 |
| arabinose | 0.6 |
| xylose | 2.7 |
| rhamnose | 0.4 |
| galacturonic acid | 2.2 |
| glucuronic acid | 0.2 |
| GGM,[a] mol % | 94 |
| degree of acetylation (DA),[b] % | 20 |
| av molar mass, kDa | 21.5 |

[a] GGM molar ratio is calculated on the summary of galactose, glucose, and mannose. [b] DA is calculated on the molar ratio of acetyl groups per GGM sugar unit.

**Determination of Monosaccharides and Oligosaccharides.** Gas chromatography (GC) and matrix-assisted laser desorption/ionization time-of-flight mass spectrometry (MALDI-TOF-MS) were used to characterize the monosaccharides and oligosaccharides after hydrolysis.

The monosaccharides were analyzed by GC on a 25 m × 0.2 mm i.d. column coated with cross-linked methyl polysiloxane (HP-1) after direct silylation of the sample (*29*). A flame ionization detector (FID) was used.

The oligosaccharides were determined by GC on a 7.5 m × 0.53 mm i.d. column coated with cross-linked methyl polysiloxane (HP-1) after direct silylation of the sample. The gas chromatography was a Perkin-Elmer AutoSystem XL instrument, and the column oven parameters were as follows: 120 °C, raised at 6 °C $min^{-1}$ to 300 °C (10 min); carrier gas, $H_2$ (20 mL $min^{-1}$); split injector (1:20), 260 °C; FID detector, 300 °C; injection volume, 1 $\mu$L. Betulinol was used as internal standard.

Hydrolysates were analyzed by MALDI-TOF-MS using an Ultraflex workstation (Bruker Daltonics, Bremen, Germany) equipped with a nitrogen laser of 337 nm and operated in a positive mode (*30*). After a delayed extraction time of 200 ns, the ions were accelerated to a kinetic energy of 12000 V and subsequently detected using reflector mode. For the MALDI-TOF-MS measurement, 2 $\mu$L of sample solution was mixed on the MALDI-TOF-plate (Bruker Daltonics) with 2 $\mu$L of matrix solution of 9 mg/mL 2,5-dihydroxybenzoic acid (Bruker Daltonics) in 30% acetonitrile and dried under a stream of air.

## RESULTS AND DISCUSSION

**Molar Mass and Molar Mass Distribution.** The sugar unit ratio was 0.6:1:3.9 (galactose/glucose/mannose) for spruce GGM. The molar mass ($M_w$) of GGM was 21.5 kDa determined by size exclusion chromatography with a multiangle laser light scattering detector. The degree of acetylation of GGM was 20%. The kinetics of the acid hydrolysis of spruce GGM was investigated by determining the molar mass distribution (MWD) and the molar mass ($M_w$) after certain reaction times.

**Figure 2** shows the evolution of MWD during acid hydrolysis of GGM at 90 °C and pH 1. A significant decrease in molar mass was observed. The peak maximum was shifted by approximately half of the magnitude already after 10 min. After

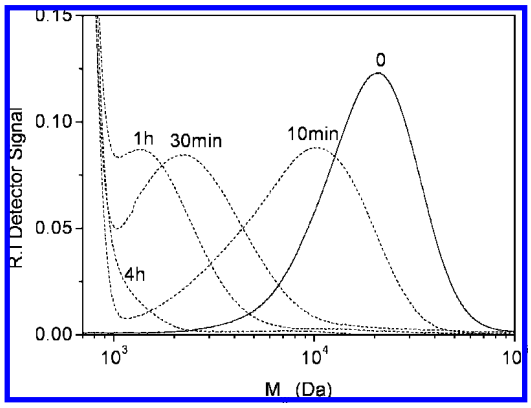


**Figure 2.** Typical $M_w$ patterns for GGM hydrolyzed for different times at 90 °C and pH 1 as measured by HPSEC. The concentration of the GGM solution was 0.4%.

2 days, no peak was detected. This is because only monomers were found. The MWD further broadened and shifted to lower molar mass with time.

**Figure 3** shows a plot of evolution in $M_n$ and $M_w$ of GGM undergoing hydrolysis as a function of reaction time. Each data point represents an independent measurement of a sample from a particular experiment, in which the solution pH was adjusted to 1, 2, or 3, respectively, at 90 °C. In the case of pH 1, both $M_w$ and $M_n$ decreased dramatically at the beginning of hydrolysis and then leveled off when polymers had been depolymerized into monomers and oligomers. The kinetics is consistent with acid hydrolysis of other polysaccharides, such as dextran (*21*). At pH 2, $M_n$ and $M_w$ decreased with time. The GGM oligomers dominated in the resulting hydrolysates. At pH 3, $M_n$ and $M_w$ decreased with time, however, leveling off after 1 day when the $M_w$ was around 10 kDa. The half-life times, $t_{1/2}$, which stands for the time when $M_w$ is decreased by half, of acid hydrolysis at 90 °C were approximately 9, 150, and 1250 min for pH 1, 2, and 3, respectively. In all applied conditions, $M_n$ was very close to $M_w$ before and after hydrolysis, which indicates a narrow distribution of molar mass. This is not common for isolated polysaccharides. This might be ascribed to a low signal-to-noise ratio of MALLS for low molar mass fractions and thereby the weak sensitivity of MALLS for oligomers. **Figure 4** shows $M_w$ of GGM undergoing hydrolysis as a function of time for the various reaction temperatures at pH 1. Compared to the $M_w$ changes at 90 °C, the changes in $M_w$ were much smaller at temperatures of 70, 50, and 37 °C. The decrease in $M_w$ at 50 °C was negligible at pH 1 after hydrolysis of 4 h and became larger after longer time. Released monosaccharides at 50 °C and pH 1 were detected after 4 h. The decrease in $M_w$ at 37 °C and lower temperatures (data not shown) was negligible over a pH range from 1 to 3, in combination with the fact that neither monosaccharides nor oligosaccharides were detected, indicating that no depolymerization occurred at 37 °C or lower temperatures.

The polydispersity, $M_w/M_n$, of GGM undergoing hydrolysis as a function of time for various reaction temperatures and pH values is shown in **Figure 5**. The $M_w/M_n$ increased with reaction time for all shown hydrolysis conditions except for hydrolysis at pH 1 and 50 °C, where no depolymerization occurred. At pH 1, the $M_w/M_n$ increased more rapidly at higher temperatures, especially at 90 °C. At 90 °C, $M_w/M_n$ increased more dramatically at pH 1 than at pH 2. This is consistent with the result of changes in $M_w$ at various temperatures and pH values. The variation in $M_w/M_n$ exhibits a good linearity as a function of time. The form of changes in $M_w/M_n$ depends on the mechanisms of chain scission (*31*). Truly random scission does not change the $M_w/M_n$. Center-favored scission will decrease the $M_w/M_n$.

**Released Monosaccharides and Oligosaccharides.** Oligosaccharides released from acid hydrolysis were identified by the mass-to-charge ratio of their sodium adducts with MALDI-TOF-MS. The mass spectrum of GGM oligomers after acid hydrolysis at 90 °C and pH 1 for 1 h showed two series of major peaks (**Figure 6A**). The major peaks with *m*/*z* number marking were the sodium adducts of hexose polymers DP3 (*m*/*z* 527), DP4 (*m*/*z* 689), DP5 (*m*/*z* 851)... to DP15 (*m*/*z* 2472). Another series of peaks with an *m*/*z* difference of 42 were oligomers carrying one acetyl group. The mass spectrum within the DP7 (*m*/*z* 1175) and DP8 (*m*/*z* 1337) range as shown in **Figure 6B** also shows the oligomers carrying one (*m*/*z* 1217, *m*/*z* 1379) or two acetyl groups (*m*/*z* 1259, 1421). The acetyl groups were reported to be located at O-2 and O-3 of mannopyranosyl units (*2, 5*). The acetyl groups were partially retained in GGM oligomers with a DP higher than 4 after acid hydrolysis even at 90 °C and pH 1, although it has been claimed that acetyl groups are easily split off at acid conditions (*32*) or, for example, during the sulfite pulping precook over a pH range of 4–7 (*33*). However, the quantitative study on the *O*-acetyl substitution in GGM molecules during acid hydrolysis will be carried on in further studies. High stability of acetyl groups is preferred to retain the GGM solubility (*4*) and also to offer the possibility of modifying the hydrolysates into new functional derivatives.

Among those oligomers, the oligomers with DP 2−5 could be quantified from data determined by GC (**Figure 7**). GGM monomers (DP1) were released in the beginning of hydrolysis and increased in amount with time during acid hydrolysis at 90 °C and pH 1. After 2 days, the monomers were the majority of GGM forms. This is inconsistent with the evolution of molar mass and molar mass distribution as shown in **Figures 2** and **3**, which imply a decrease in molar mass. GGM oligomers were released and increased in amount during the first hour (DP 3–5) or 4 h (DP 2), but decreased afterward.

**Hydrolysis Kinetics.** The reaction rate functions can be applied to interpret the time-dependent MWD patterns by obtaining the reaction order of the acid hydrolysis. Earlier studies on different polysaccharides have shown that the acid hydrolysis reaction follows the first-order kinetics (*34, 35*), given as

$$dL/dt = -kL \quad (1)$$

in which $L$ denotes the total number of hydrolyzable bonds. Therefore, the reaction rate is defined as $-dL/dt$, proportional to $L$ with a rate constant $k$. The total number of hydrolyzable bonds at the reaction time $t$ is described as

$$L_t = N_t(M_t/m - 1) \quad (2)$$

in which $M_t$ denotes the average molar mass, $m$ the monomer molar mass, and $N_t$ the number of molecules. If $M/m \gg 1$, the relationship between molar mass and hydrolysis time can be derived

$$1/M_t = 1/M_0 + kt/m \quad (3)$$

in which $M_t$ and $M_0$ are the molar masses at time $t$ and zero, respectively.

**Figure 8** presents the reciprocal of $M_w$ plotted as a function of depolymerization time for acid hydrolysis of GGM at pH 1. It shows a linear relationship between inverse $M_w$ and depolymerization time, which is consistent with eq 3. Therefore, first-order kinetics should be applied in this case. This suggests that GGM chains are randomly cleaved during acid hydrolysis

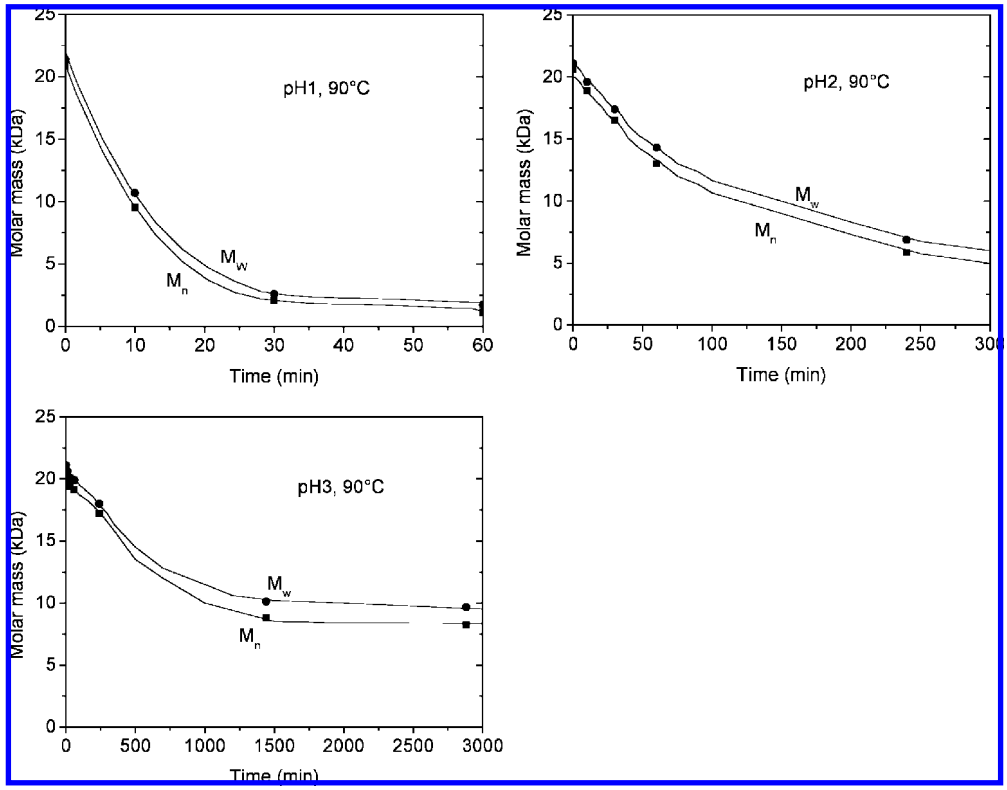


**Figure 3.** Evolution in time of $M_n$ and $M_w$ of GGM at 90 °C and pH 1−3.

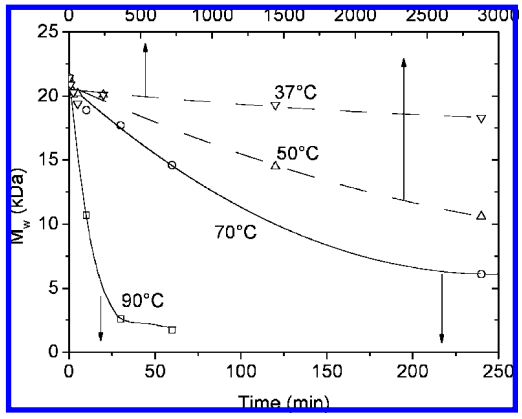


**Figure 4.** Effect of reaction time and temperature on $M_w$ by hydrolysis of GGM at pH 1. Note the different time scales. Arrows indicate the abscissa axis that belongs to the curve.

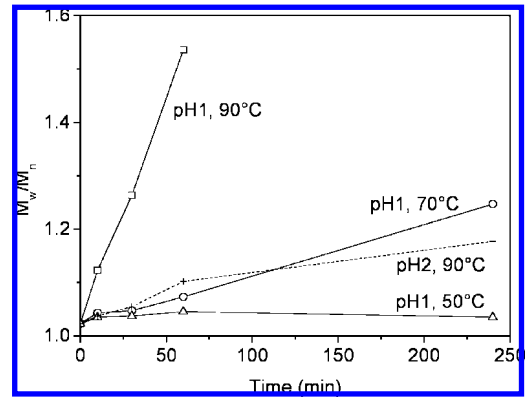


**Figure 5.** Evolution in time of $M_w/M_n$ during acid hydrolysis of GGM at different pH values and temperatures.

(*34, 36*). The resulting parameters from the plotting and equation are listed in **Table 2**. At pH 1, the apparent rate constant, $k_w$, at 90 °C was 1.51E+00, which is much higher than the value at 70 °C. When the temperature was lowered to 50 °C, the apparent rate constant $k_w$ was decreased significantly. The apparent rate constant $k_w$ at pH 2 at 90 °C was 6.67E−02. At pH >1, the apparent rate constant $k$ was much lower. The rate constant varies with different polysaccharides and the method of hydrolysis (*21, 34, 36*).

The apparent rate constant $k_w$ is temperature- and pH-dependent. The apparent rate constant $k_w$ can be rewritten to $k_0k(T)$ in which $k_0$ is independent of the temperature, $k(T)$, a function of $T$.

$$1/M_t = 1/M_0 + k_{w0}k_w(T)t/m \quad (4)$$

**Temperature Dependence of the Rate Constant.** Temperature is critical to the reaction rate constant. The changes in $M_w$ are different at various temperatures (**Figure 5**). The temperature dependence of reaction constant $k_w$ is given by the Arrhenius equation

$$k_{w0}k_w(T) = A\,e^{-E/RT} \quad (5)$$

in which $E$ is the activation energy of the reaction, $T$ the absolute temperature, $A$ the pre-exponential factor written as independent of temperature, and $R$ the universal gas constant (8.314 J mol$^{-1}$ K$^{-1}$).

The reaction rate constant during acid hydrolysis of GGM at pH 2 versus temperature 9s plotted in **Figure 9a**. The rate constant increased with temperature. The plot was fit to an exponential curve as described by the Arrhenius equation. The rate constant should reach a maximum value $A_0$. Activation energy was determined from the data on the temperature dependence of reaction constant by graphical analysis of eq 5.

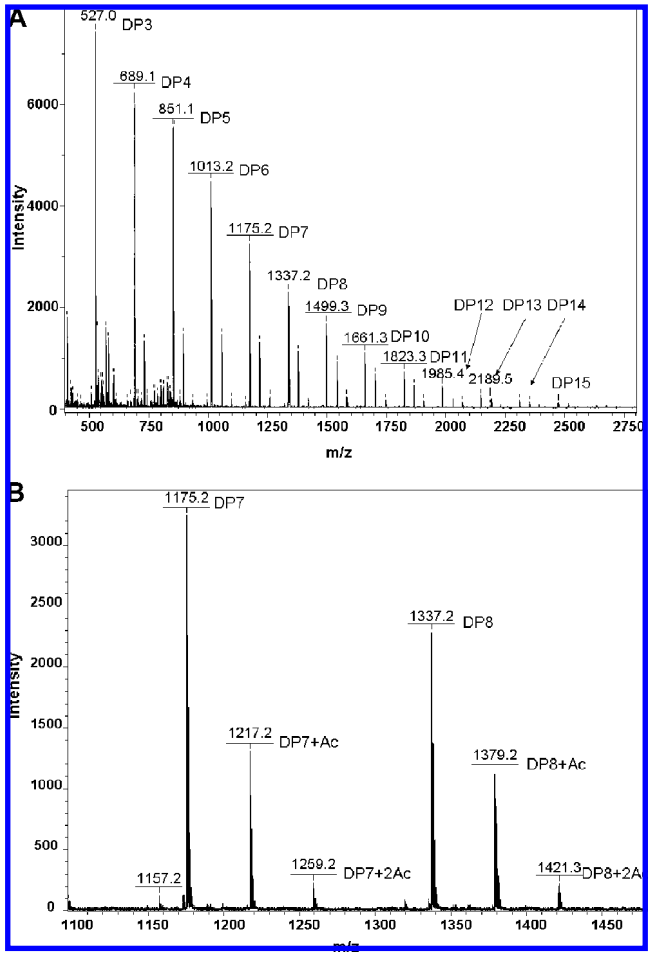


**Figure 6.** (**A**) Full-scale MALDI-TOF mass spectrum of GGM oligomers after acid hydrolysis at 90 °C and pH 1 for 1 h. (**B**) Zoom of (**A**) with a range from 1100 to 1500 *m/z*. Ac indicates one *O*-acetyl substituent and 2Ac two *O*-acetyl substituents.

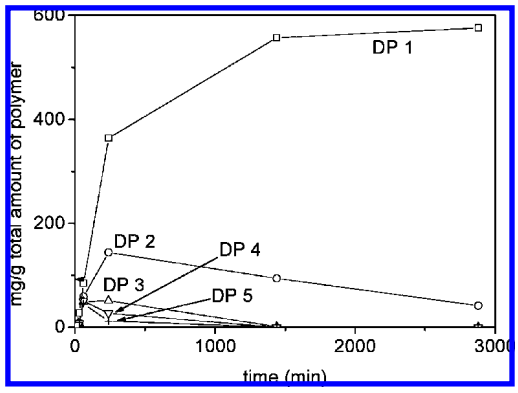


**Figure 7.** Released mono- (DP1) and oligosaccharides with a DP of 2−5 during acid hydrolysis at 90 °C and pH 1, determined by GC.

In most cases, however, $A_0$ is not always detectable. By taking logarithms of both sides, eq 5 is written to

$$\ln K_w = -E/RT + \ln A \quad (6)$$

Therefore, the plot of the natural logarithm of the rate constant versus the reciprocal of temperature is linear with a slope of $-E/R$ and an intercept of ln $A$, as shown in **Figure 9b**. Its linearity confirmed that $A$ is independent of temperature. The estimated parameters are listed in **Table 3**. Activation energy $E$ was extracted from the slope of the Arrhenius plot. The value of $E$ was 150.3 kJ mol$^{-1}$ during acid hydrolysis at pH 1. This

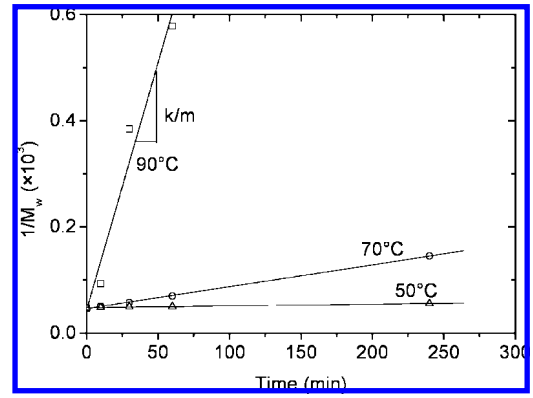


**Figure 8.** Reciprocal of $M_w$ plotted as a function of depolymerization time at 90 °C.

value was much higher than that of κ-carrageenan for acid hydrolysis under different conditions (i.e., 113.1 kJ mol$^{-1}$ in 0.09 mol L$^{-1}$ LiCl, 0.01 mol L$^{-1}$ HCl buffer at pH of 2) (*34*) and that of chitosan for nitrous acid hydrolysis (87.1 kJ mol$^{-1}$) or alkaline hydrolysis (92 kJ mol$^{-1}$) (*36, 37*). The activation energy of acid hydrolysis of GGM was also higher than that of acid hydrolysis of methyl pyranosides with 0.5 M acid at 60–90 °C for each monomer (*25*). In general, acid hydrolysis of polysaccharides is influenced by their structures, conformation of individual sugar units, and acidic medium. The hydrolysis rate of β-anomers is higher than that of corresponding α-anomers (*25*). It increases in the order glucoside, mannoside, galactoside, xyloside, and arabinoside. The activation energy $E$ for acid hydrolysis of GGM at pH 2 was found to be equal to that of pH 1. The independence of the reaction pH was also reported in the acid hydrolysis of oligofructose samples (*28*).

Furthermore, eq 4 can be written to

$$1/M_t = 1/M_0 + A\,e^{-E/RT}t/m \quad (7)$$

Here, activation energy $E$ for acid hydrolysis of GGM is 150.3 kJ mol$^{-1}$.

**Influence of Reaction pH.** A kinetic study on acid hydrolysis of inulin and oligofructose (*28*) claimed that the rate constant of hydrolysis was independent of the acid type and dependent only on the proton concentration [H$^+$].

**Figure 10a** shows the evolution of the reaction rate constant for acid hydrolysis of spruce GGM as a function of [H$^+$] at 90 °C. The reaction rate constant during acid hydrolysis at 90 °C was directly proportional to [H$^+$]. The double-logarithmic plot of the reaction rate constant as a function of the H$^+$ concentration during hydrolysis at 90 °C gives a straight line with a slope of approximately 1. It indicates a first order with respect to [H$^+$] at 90 °C over the studied pH range.

Therefore, the relationship between the reaction rate constant and [H$^+$] during acid hydrolysis can be described by

$$k_w(\mathrm{pH}) = k_y^0 + k_w^0[\mathrm{H}^+] = k_y^0 + k_w^0 \times 10^{-\mathrm{pH}} \quad (8)$$

in which $k_w$(pH) is a linear function of [H$^+$] or $10^{-\mathrm{pH}}$ with a slope of $k_w^0$ and intercept of $k_y^0$.

It was found that acid hydrolysis at 70 °C resulted in a linear relationship with the same slope. This means that, regardless of temperature, the reaction rate constant during acid hydrolysis increased for acid hydrolysis at 90 °C by a factor of 10 with a decrease in pH by 1 unit or an increase in [H$^+$] by 10. Blecker et al. (*28*) reported the same factor by reaction pH for acid hydrolysis of oligofructose.

**Table 2.** Analysis of $M_w$ Data by Equation 3

| | pH 1 | | | pH 2 | | | pH 3 | | |
|---|---|---|---|---|---|---|---|---|---|
| reaction temp, °C | $M_w(0)$,[a] kDa | $k_w$,[b] min$^{-1}$ | $R^2$ | $M_w(0)$, kDa | $k_w$, min$^{-1}$ | $R^2$ | $M_w(0)$, kDa | $k_w$, min$^{-1}$ | $R^2$ |
| 90 | 23.5 | 1.51E + 00 | 0.967 | 21.6 | 6.67E − 02 | 0.999 | 19.8 | 3.47E − 03 | 0.892 |
| 70 | 22.6 | 8.00E − 02 | 0.994 | 20.9 | 4.56E − 03 | 0.998 | | | |
| 50 | 21.0 | 2.58E − 03 | 0.994 | | | | | | |

[a] $M_w(0)$ denotes the molar mass at time zero. [b] $k_w$ denotes the rate constant.

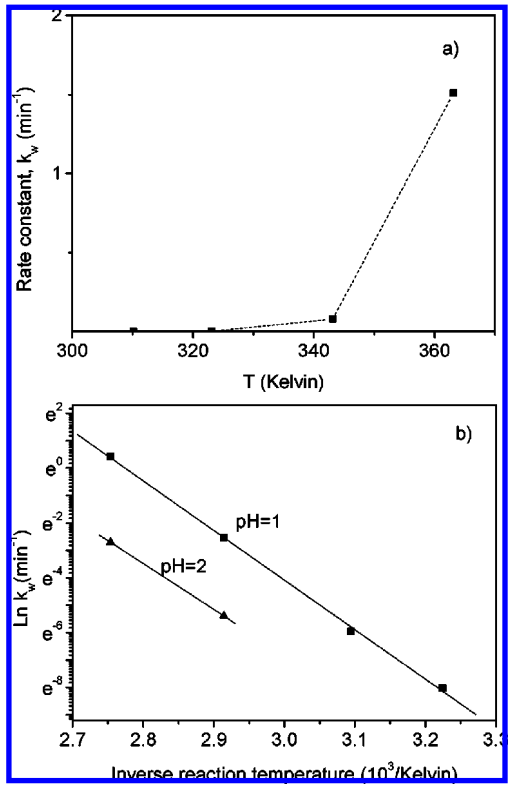


**Figure 9.** (**a**) Arrhenius plot for the reaction rate constant $k_m$ and reaction rate constant dependence on temperature for acid hydrolysis of GGM at pH of 1. (**b**) Form of Arrhenius plot for determination of activation energy for acid hydrolysis of GGM at pH of 1 (■) and 2 (▲).

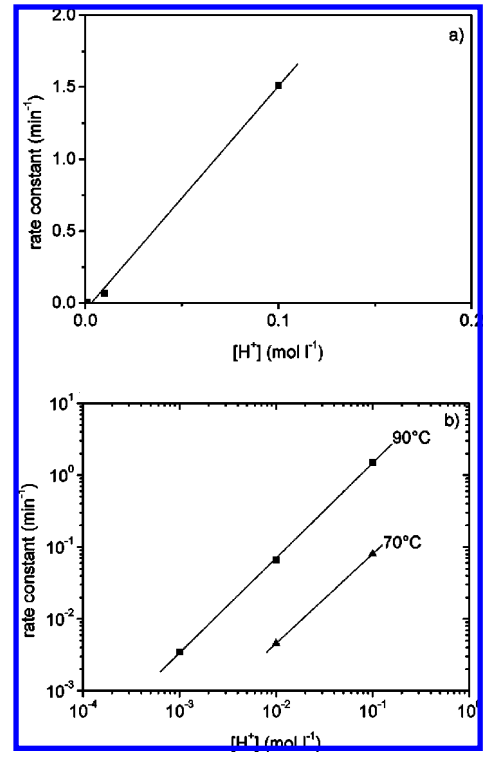


**Figure 10.** (**a**) Reaction rate constant as a function of $H^+$ concentration during hydrolysis at 90°. (**b**) Double logarithmic plot of reaction rate constant as a function of $H^+$ concentration during hydrolysis at 90 °C (■) and 70 °C (▲).

**Table 3**

(**A**) Estimated Activation Energy for the Hydrolysis Process

| | $A$, min$^{-1}$ | $E$, kJ mol$^{-1}$ | $R^2$ |
|---|---|---|---|
| molar mass $k_w$, eq 6 | 6.09E + 21 | 150.3 | 0.999 |

(**B**) Activation Energy for Acid Hydrolysis of Methyl Pyranosides with 0.5 M Acid at 60–90 °C (*25*)

| | $E$, kJ mol$^{-1}$ | |
|---|---|---|
| | α-anomer | β-anomer |
| D-glucose | 147.0 | 136.1 |
| D-mannose | 145.3 | |
| D-galactose | 142.4 | 134.0 |

Therefore, considering the effect of temperature and pH condition, eq 7 can be written to

$$1/M_t = 1/M_0 + (k_1 + k_2 \times 10^{-\mathrm{pH}})\mathrm{e}^{-E/RT}t/m \qquad (9)$$

in which $k_1$ and $k_2$ are constants regardless of temperature and pH condition.

The reaction kinetics for acid hydrolysis of GGM can also be discussed by investigating the release of GGM monomers and oligomers. As plotted in **Figure 7**, the initial rate constant $k_{i,t=0}$ of each resultant of reaction during acid hydrolysis at 90 °C and pH 1 was observed to be different. The $k_{i,t=0}$ for GGM oligomers with DP 2–5 was in the range of 0.3–0.5 mg/g·min. This indicates that the GGM molecule chains were cleaved by random scission. The apparent rate constant for each resultant first increased for a short treatment period, but then decreased. The total number of hydrolyzable bonds and the molar masses are discussed for the purpose of kinetic studies in general and in the current paper, although the observation of released monomers and oligomers is important in studies on the mechanism of acid hydrolysis.

## LITERATURE CITED

(1) Sjöström, E. Wood polysaccharides. In *Wood Chemistry—Fundamentals and Applications*, 2nd ed.; Academic Press: San Diego, CA, 1993; pp 49.

(2) Willför, S.; Sjöholm, R.; Laine, C.; Roslund, M.; Hemming, J.; Holmbom, B. Characterisation of water-soluble galactoglucomannans from Norway spruce wood and thermomechanical pulp. *Carbohydr. Polym.* **2003**, *52*, 175–187.

(3) Willför, S.; Sundberg, A.; Hemming, J.; Holmbom, B. Polysaccharides in some industrially important softwood species. *Wood Sci. Technol.* **2005**, *39*, 245–258.

(4) Willför, S.; Sundberg, K.; Tenkanen, M.; Holmbom, B. Spruce-derived mannans—a potential raw material for hydrocolloids and novel advanced natural materials *Carbohydr. Polym.* **2008**, 10.1016/j.carbopol.2007.08.006.
(5) Hannuksela, T.; du Penhoat, C. H. NMR structural determination of dissolved O-acetylated galactoglucomannan isolated from spruce thermomechanical pulp. *Carbohydr. Res.* **2004**, *339*, 301–312.
(6) Stålbrand, H.; Lundqvist, J.; Andersson, A.; Hägglund, P.; Anderson, L.; Tjerneld, F.; Jacobs, A.; Teleman, A.; Dahlman, O.; Palm, M.; Zacchi, G. Isolation, characterization, and enzymatic hydrolysis of acetyl-galactoglucomannan from spruce (*Picea abies*). In *Hemicelluloses: Science and Technology*; Gatenholm, P., Tenkanen, M., Eds.; ACS Symposium Series 864; American Chemical Society: Washington, DC,2004; pp 66.
(7) van Hazendonk, J. M.; Reinerink, E. J. M.; de Waard, P.; van Dam, J. E. G. Structral analysis of acetylated hemicellulose polysaccharides from fibre flax (*Linum usitatissimum* L.). *Carbohydr. Res.* **1996**, *291*, 141–145.
(8) Willför, S.; Rehn, P.; Sundberg, A.; Sundberg, K.; Holmbom, B. Recovery of water-soluble acetyl-galactoglucommans from mechanical pulp of spruce. *Tappi J.* **2003**, *2*, 27–32.
(9) Persson, T.; Nordin, A.-R.; Zacchi, G.; Jönsson, A.-S. Economic evaluation of isolation of hemicelluloses from process streams from thermomechanical pulping of spruce. *Appl. Biochem. Biotechnol.* **2007**, *741*, 136–140.
(10) Hannuksela, T.; Tenkanen, M.; Holmbom, B. Sorption of dissolved galactoglucomannans and galactomannans to bleached kraft pulp. *Cellulose* **2002**, *9* (3–4), 251–261.
(11) Söderqvist-Lindblad, M.; Albertsson, A. C.; Ranucci, E.; Laus, M.; Giani, E. Biodegradable polymers from renewable sources: rheological characterization of hemicellulose-based hydrogels. *Biomacromolecules* **2005**, *6*, 684–690.
(12) Mikkonen, K.; Helen, H.; Talja, R.; Willför, S.; Holmbom, B.; Hyvönen, L.; Tenkanen, M. Advances in Chemistry and Processing of Lignocellulosics. In *Proceedings of European Workshop on Lignocellulosics and Pulp*, University of Natural Resources and Applied Life Sciences Vienna (BOKU); Vienna, Austria, 2006; pp 130–133.
(13) Hartman, J.; Albertsson, A. C.; Sjöberg, J. Surface- and bulk-modified galactoglucomannan hemicellulose films and film laminates for versatile oxygen barriers. *Biomacromolecules* **2006**, *7*, 1983–1989.
(14) Ebringerová, A.; Hromádková, Z.; Høríbalová, V.; Xu, C.; Holmbom, B.; Sundberg, A.; Willför, S. Norway spruce galactoglucomannans exhibiting immunomodulating and radical-scavenging activities. *Int. J. Biol. Macromol.* **2008**, *42*, 1–5.
(15) Xu, C.; Willför, S.; Sundberg, K.; Pettersson, C.; Holmbom, B. Physicochemical characterization of spruce galactoglucomannans: solubility, stability, surface activity, and rheology. *Cell. Chem. Technol.* **2007**, *41* (1), 55–65.
(16) Soldi, V. Stability and degradation of polysaccharides. In *Polysaccharides Structural Diversity and Functional Versatility*, 2nd ed.; Dumitriu, S., Ed.; Dekker: New York, 2005; pp 395.
(17) Shahidi, F.; Arachchi, J. K. V.; Jeon, Y. J. Food applications of chitin and chitosans. *Trends Food Sci. Technol.* **1999**, *10*, 37–51.
(18) Wyman, C. E.; Decker, S. R.; Himmel, M. E.; Brady, J. W.; Skopec, C. E.; Viikari, L. Hydrolysis of cellulose and hemicellulose. In *Polysaccharides Structural Diversity and Functional Versatility*, 2nd ed.; Dumitriu, S., Ed.; Dekker: New York, 2005; pp 995.
(19) Miyazawa, T.; Funazukuri, T. Polysaccharide hydrolysis accelerated by adding carbon dioxide under hydrothermal conditions. *Biotechnol. Prog.* **2005**, *21*, 1782–1785.
(20) Palmarola-Adrados, B.; Juhász, T.; Galbe, M.; Zacchi, G. Hydrolysis of nonstarch carbohydrates of wheat-starch effluent for ethanol production. *Biotechnol. Prog.* **2004**, *20*, 474–479.
(21) Basedow, A. M.; Ebert, K. H.; Ederer, H. J. Kinetic studies on the acid hydrolysis of dextran. *Macromolecules* **1978**, *11*, 774–781.
(22) Cheetham, N. W. H.; Mashimba, E. N. M. Characterization of some enzymatic hydrolysis products of xanthan. *Carbohydr. Polym.* **1991**, *15* (2), 195–206.
(23) Cote, G. L.; Willet, J. L. Thermomechanical depolymerization of dextran. *Carbohydr. Polym.* **1999**, *39* (2), 119–126.
(24) Chen, R. H.; Chang, J. R.; Shyur, J. S. Effects of ultrasonic conditions and storage in acidic solutions on changes in molar mass and polydispersity of treated chitosan. *Carbohydr. Res.* **1997**, *299* (4), 287–294.
(25) Lai, Y.-Z. Chemical degradation. In *Wood and Cellulosic Chemistry*, 2nd ed.; Hon, D. N.-S., Shiraishi, N., Eds.; Dekker: Basel, Switzerland, 2001; pp 443.
(26) Tayal, A.; Kelly, R. M.; Khan, S. A. Rheology and molecular weight changes during enzymatic degradation of a water-soluble polymer. *Macromolecules* **1999**, *32*, 294–300.
(27) Tayal, A.; Khan, S. A. Degradation of a water-soluble polymer: molecular weight changes and chain scission characteristics. *Macromolecules* **2000**, *33*, 9488–9493.
(28) Blecker, C.; Fougnies, C.; van Herck, J.-C.; Chevalier, J.-P.; Paquot, M. Kinetic study of the acid hydrolysis of various oligofructose samples. *J. Agric. Food Chem.* **2002**, *50*, 1602–1607.
(29) Sundberg, A.; Sundberg, K.; Lillandt, C.; Holmbom, B. Determination of hemicelluloses and pectins in wood and pulp fibres by acid methanolysis and gas chromatography. *Nord. Pulp Pap. Res. J.* **1996**, *11*, 216–219.
(30) Hilz, H.; Jong, L. E.; Kabel, M. A.; Schols, H. A.; Voragen, A. G. J. A comparison of liquid chromatography, capillary electrophoresis, and mass spectrometry methods to determine xyloglucan structures in black currants. *J. Chromatogr., A* **2006**, *1133*, 275–286.
(31) Emsley, A. M.; Heywood, R. J. Computer modeling of the degradation of linear polymers. *Polym. Degrad. Stab.* **1995**, *45*, 145–149.
(32) Vuorinen, T.; Alén, R. Carbohydrates. In *Analytical Methods in Wood Chemistry, Pulping and Papermaking*; Sjöström, E., Alén, R., Eds.; Springer: Heidelberg, Germany, 1999; pp 38–71.
(33) Croon, I.; Enstrom, B.; Rydholm, S. *Svensk Papperstid.* **1964**, *67* (5), 196–199.
(34) Singh, S. K.; Jacobsson, S. P. Kinetics of acid hydrolysis of κ-carrageenan as determined by molar mass (SEC-MALLS-RI), gel breaking strength, and viscosity measurements. *Carbohydr. Polym.* **1994**, *23*, 89–103.
(35) Simha, R. Kinetics of degradation and size distribution of long chain polymers. *J. Appl. Phys.* **1941**, *12*, 569–578.
(36) Chang, K. L. B.; Tai, M.-C.; Cheng, F. H. Kinetics and products of degradation of chitosan by hydrogen peroxide. *J. Agric. Food Chem.* **2001**, *49*, 4845–4851.
(37) Allan, G. G.; Peyron, M. Molar mass manipulation of chitosan I: kinetics of depolymerization by nitrous acid. *Carbohydr. Res.* **1995**, *277*, 257–272.

**Received for review December 19, 2007. Revised manuscript received January 31, 2008. Accepted January 31, 2008. This work was financed by the Academy of Finland (FA 207091), which is gratefully acknowledged. This work is part of the activities at the Åbo Akademi Process Chemistry Centre within the Finnish Centre of Excellence Programme (2000−2011) by the Academy of Finland and also part of the activities within the EPNOE network (European Polysaccharide Network of Excellence). Part of the work was done within the EU Project WaCheUp (EU STREP 013896).**

JF703702Y